Int. J. Electrochem. Sci., 12 **(2017)** 10259 – 10268, doi: 10.20964/2017.11.100

International Journal of
ELECTROCHEMICAL
SCIENCE
www.electrochemsci.org

Preparation and Corrosion Resistance of Ni–W–Y_2O_3–ZrO_2 Nanocomposite Coatings

Qingwei Niu[1], *Zili Li*[1*], *Xiaofeng Yan*[2], *Guodong Liu*[3], *Bingying Wang*[3]

[1] College of Pipeline and Civil Engineering, China university of petroleum (East China), Qingdao, China, 266580
[2] The Sixth Gas Production Plant in Changqing Oilfield, Xi'an, China, 710018
[3] College of Mechanical and Electronic Engineering, China university of petroleum (East China), Qingdao, China, 266580
[*]E-mail: zilimenhuzu@163.com

Received: 15 July 2017 / *Accepted:* 6 September 2017 / *Published:* 12 October 2017

Composite coatings containing Y_2O_3 and ZrO_2 nanoparticles were prepared by the composite electrodeposition technique under ultrasonic stirring and electromagnetic stirring. The microstructure of the nanocomposite coatings was observed by scanning electron microscopy. In addition, the microhardness of the nanocomposite coatings was tested. Electrochemical polarization curves and AC impedance spectra of the nanocomposite coatings were tested in 3.5 wt% NaCl solution to study the corrosion resistance. The experimental results showed that the composite coatings prepared under ultrasonic stirring were compact, fine grain, and had no cracks. Compared to Ni–W alloy coating, the addition of nanoparticles Y_2O_3 and ZrO_2 significantly improved the microhardness and corrosion resistance of the composite coatings.

Keywords: Composite coating; Y_2O_3; ZrO_2; Nanoparticles; Corrosion resistance

1. INTRODUCTION

Nickel-based composites have been widely used in automotive and aerospace fields owing to their good corrosion resistance and high-temperature mechanical properties [1–5]. Tungsten has the characteristics of high hardness and good chemical stability, and its melting point is also the highest in natural metals. Chromium can cause serious environmental pollution. However, the activity of tungsten is lower than that of chromium, and it does not cause environmental pollution. It is well known that tungsten cannot be deposited separately from the solution, because of the negative potential [6]. However, using depolarization and induction of iron, nickel, and other iron elements, nickel and tungsten can be co-deposited forming nickel–tungsten alloy [7]. Nickel–tungsten (Ni–W) alloy has

higher hardness and corrosion resistance and is more environmentally friendly compared to chromium coating.

It has been reported that the incorporation of nanoparticles and the use of ultrasound can improve the grain and the performance of coating [8–11]. ZrO_2 nanoparticle has the characteristics of high hardness, high strength, high melting point, excellent thermal stability and good chemical resistance. It has been applied in the fields of mechanical, electronic, refractory, and ceramics. The Ni–ZrO_2 nanocomposite coating prepared by adding ZrO_2 nanoparticles to the electroplating solution has excellent high temperature oxidation resistance [12]. Using rotating cathodes, Ni–ZrO_2 nanocomposite coatings prepared by ultrasonic pulse electrodeposition have a more uniform microstructure, denser particles, and excellent corrosion resistance than pure nickel coatings [13]. Y_2O_3 is a type of new rare-earth material with a high corrosion resistance and high temperature stability. It has been applied to phosphor, optical glass, oxygen sensor, ceramic, and high-temperature superconducting material. Ni–W–Y_2O_3–ZrO_2 nanocomposite coating prepared under ultrasonic stirring have shown smaller grain size, higher microhardness, better oxidation resistance, and abrasion resistance [14,15].

In this study, Ni–W–ZrO_2, Ni–W–Y_2O_3, and Ni–W–Y_2O_3–ZrO_2 composite coatings were prepared by the composite electrodeposition technique on N80 steel plates. AC impedance spectroscopy and potentiodynamic polarization curve of the composite coatings were tested in 3.5 wt% NaCl solution. In addition, the composite coatings were also characterized by scanning electron microscopy (SEM), energy dispersive spectroscopy (EDS) analysis, and microhardness test.

2. EXPERIMENTAL

2.1. Electrodeposition

Table 1. Composition and content of the alkaline washing solution

Composition	NaOH	Na_2CO_3	Na_3PO_4	Na_2SiO_3
Content (g/L)	20	20	10	10

During the electrodeposition process, a pure nickel plate was used as the anode, whereas N80 steel plate (30 mm × 20 mm × 3 mm) was used as the cathode. Before electrodeposition, one side of the cathode plate was mechanically polished to get a smooth, bright, and uniform surface, and the other five sides were encapsulated in silicone. Then, the cathode was put in an alkaline washing solution for 10 min to remove the oil on the surface. The composition and content of the alkaline washing solution were listed in Table 1. After caustic washing, the cathode was activated by the mass fraction of 10% dilute hydrochloric acid. The composition and content of the base bath during the composite electrodeposition were listed in Table 2. When only one type of nanoparticle was added into the plating bath, the addition amount of ZrO_2 or Y_2O_3 nanoparticles was 10 g/L. When ZrO_2 and Y_2O_3 nanoparticles were added together, the addition amount of ZrO_2 and Y_2O_3 nanoparticles was 5 g/L, respectively. To prevent agglomeration of nanoparticles, the plating bath was electromagnetically

stirred at 500 rpm for 2 h. The pH of the solution was adjusted to ~7 using citric acid and ammonia. The average current density was 1.5 A/dm^2, and the temperature was kept at 60 °C. The ultrasonic stirring was carried out at 45 kHz and 300 W for 2 h.

Table 2. Composition and concentration of the plating solution

Composition	$NiSO_4$	$Na_3C_6H_5O_7$	Na_2WO_4	$NiCl_2$
Concentration (g/L)	50	80	60	10

2.2. Electrochemical corrosion test

The CS310 electrochemical workstation was used to test the AC impedance and the potential polarization curve. The experiment was carried out at room temperature. 3.5% NaCl solution was used as the corrosion solution. All the experiments were conducted using typical three-electrode electrochemical cells. A saturated calomel electrode and a graphite rod were used as the reference and counter electrodes, respectively. The working electrode was Ni–W alloy coating or composite coating, leaving an area of 1 cm^2 exposed to the solution. Impedance spectra were recorded in the frequency range 10^5–10^{-2} Hz, and the starting potential was the open circuit potential. Polarization curves were recorded in the potential range ±250 mV vs. open circuit potential at a scan rate of 0.166 mV/s.

2.3. Microhardness test

The microhardness of the composite coating was measured using an HV-1000A microhardometer at a load of 200 g. The loading time was 15 s, and the result was the average value of five points.

3. RESULTS AND DISCUSSION

3.1. SEM study

Ni–W–ZrO_2, Ni–W–Y_2O_3, and Ni–W–Y_2O_3–ZrO_2 composite coatings were prepared under ultrasonic stirring and electromagnetic stirring. The SEM images of the surface morphology and cross-section SEM images of the coatings were shown in Figs. 1 and 2, respectively. Through the comparison of the surface morphology of the composite coatings under two types of stirring methods, the surface of the composite coatings prepared under ultrasonic stirring was found to be compact with small grain size [16]. The surface uniformity of the composite coating prepared under the electromagnetic stirring was poor, accompanied by the occurrence of more serious cracking phenomenon.

The boundary between the coating and the substrate was shown obviously in Fig. 2. Fig. 2(a) showed that the surface undulating of the coating prepared under the condition of electromagnetic stirring was larger. However, Fig. 2(b) showed that the surface roughness of the coating prepared

under ultrasonic stirring was very good. Figs. 2(c) and 2(d) were photographs of cracks and pinholes, respectively. Zhu *et al*. reported that the cracks in the composite coating occurred because of hydrogen embrittlement. Near the cathode, in addition to the reduction of nickel ions, hydrogen ions also react to generate hydrogen gas, resulting in hydrogen embrittlement. Because the intensity of ultrasonic stirring is much higher than that of electromagnetic stirring, the hydrogen produced can be taken away from the cathode surface in time, reducing the effect of hydrogen embrittlement. However, the strength of electromagnetic stirring is lower, and the generated hydrogen cannot be taken away from the cathode surface immediately, thus increasing the brittleness of the composite coating and forming cracks.

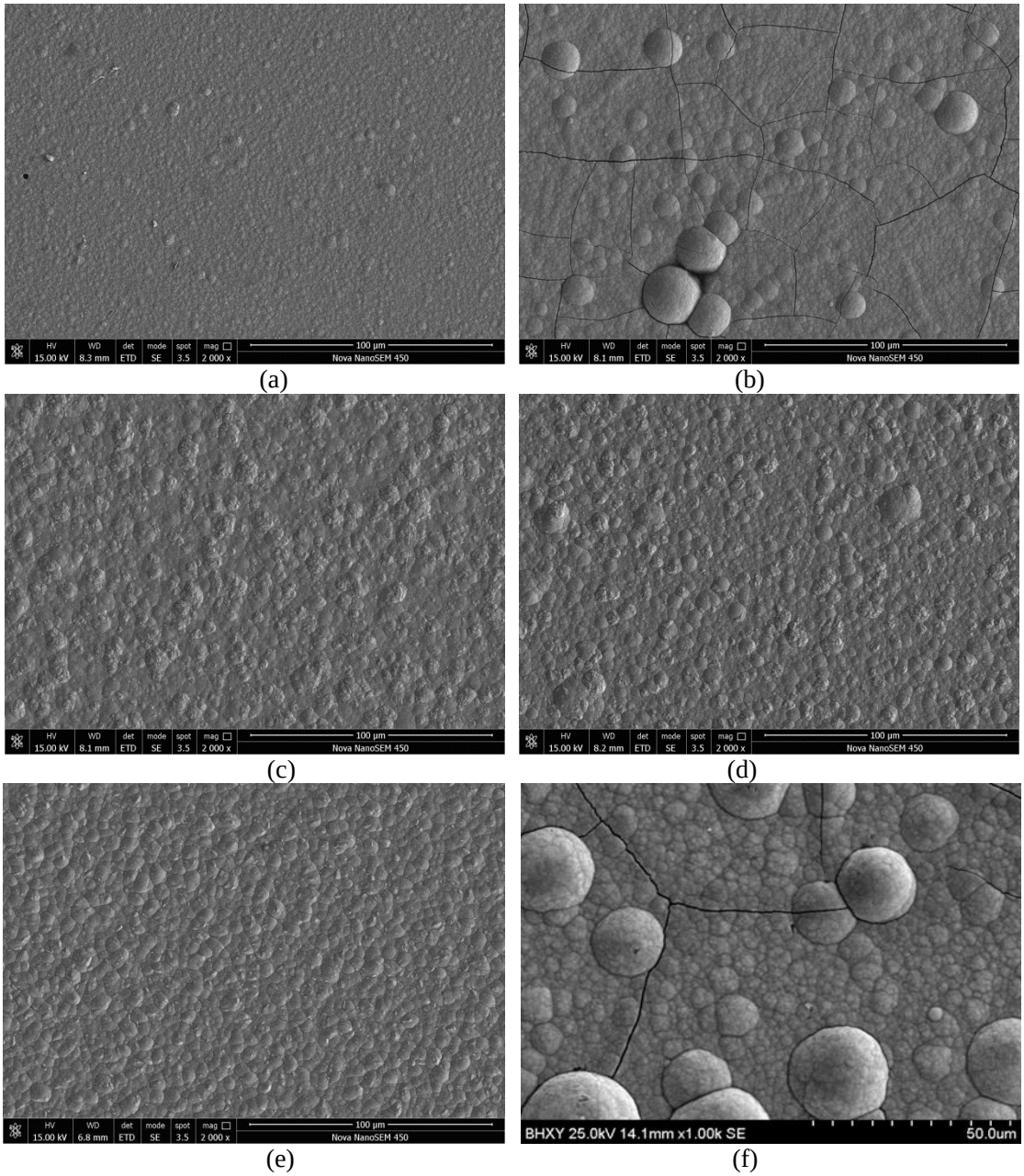

Figure 1. SEM images of composite coatings: (a) Ni–W–ZrO_2, ultrasonic stirring (b) Ni–W–ZrO_2, electromagnetic stirring (c) Ni–W–Y_2O_3, ultrasonic stirring (d) Ni–W–Y_2O_3, electromagnetic stirring (e) Ni–W–Y_2O_3–ZrO_2, ultrasonic stirring (f) Ni–W–Y_2O_3–ZrO_2, electromagnetic stirring

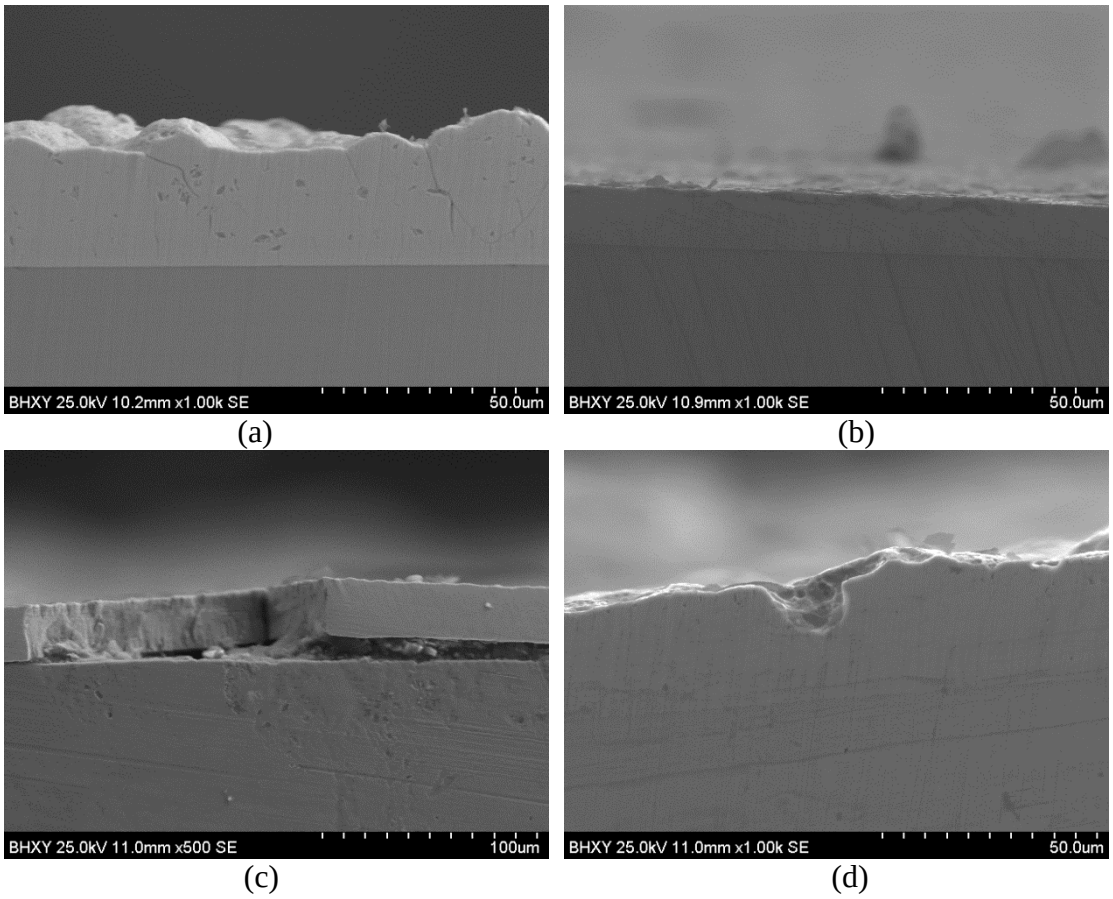

Figure 2. Sectional SEM of composite coatings: (a) electromagnetic stirring (b) ultrasonic stirring (c) crack across the coating (d) pinhole on the surface of the coating

3.2. EDS analysis

The EDS results of the corresponding positions of the composite coating were shown in Fig. 3. The contents of each element were listed in Table 3. The presence of Zr and Y in the composite coating indicated that the insoluble nanoparticles in the plating solution can be co-deposited with nickel ions into the composite coating. Compared to other studies, the reason for the low content of nanoparticles in the composite coating might be the lower current density during the electrodeposition process [18]. The reason for using a small current density (1.5 A/dm^2) was based on our previous study, where the current density of 1.5 A/dm^2 was the optimum current parameter for the preparation of Ni–W alloy coating. When the current density was 1 A/dm^2, the center and surrounding of the coating were uneven, because of the edge effect of the current. However, at a current density of 2 A/dm^2, there were many cracks on the edge of the coating and a few cracks in the center. No crack and unevenness in the coating were observed at a current density of 1.5 A/dm^2.

Table 3 showed that when the two types of nanoparticles were added simultaneously, the total content of nanoparticles in the composite coating became a little lower than that of Ni–W–ZrO_2 and Ni–W–Y_2O_3 composite coating. This may be due to the increased chance of collision and

agglomerating between the two nanoparticles in the bath, thereby reducing the total amount of nanoparticles deposited in the coating.

Table 3. Element content of Ni–W composite coatings containing ZrO_2 and Y_2O_3

at（%）	O	Ni	W	Zr	Y
Ni–W–Y_2O_3	6.8	80.69	11.67	--	0.84
Ni–W–ZrO_2	7.73	80.14	11.15	0.98	--
Ni–W–Y_2O_3–ZrO_2	5.31	81.91	11.97	0.42	0.39

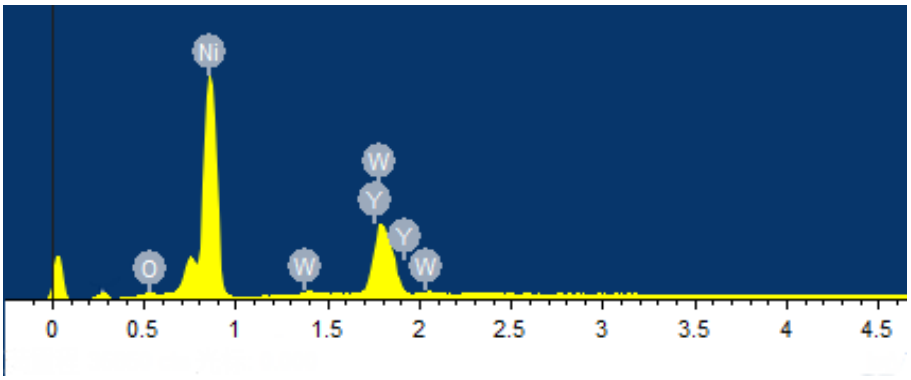

(a)

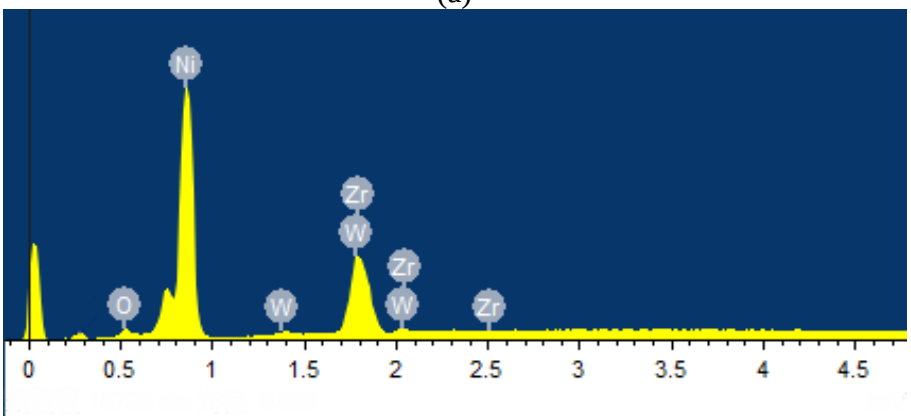

(b)

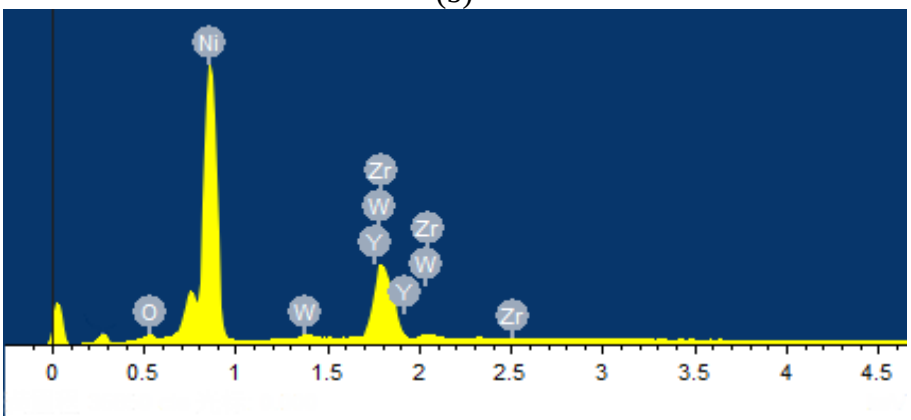

(c)

Figure 3. The EDS of (a) Ni–W–Y_2O_3 composite coating (b) Ni–W–ZrO_2 composite coating (c) Ni–W–Y_2O_3–ZrO_2 composite coating

3.3. Microhardness test

The comparison results of microhardness between the composite coatings and the Ni–W alloy coating without nanoparticles were shown in Fig. 4. The microhardness of Ni–W alloy coating was 346.74 $HV_{0.2}$. The microhardness of Ni–W–ZrO_2 and Ni–W–Y_2O_3 composite coating after adding nanoparticles obviously increased to 549.69 and 518.3$HV_{0.2}$, respectively. However, the microhardness of the Ni–W–Y_2O_3–ZrO_2 composite coating obtained after the addition of the two types of nanoparticles was 524.82 $HV_{0.2}$, which was between those of Ni–W–ZrO_2 and Ni–W–Y_2O_3 composite coatings. The content of added nanoparticles will be further optimized. Compared to literature [19–21], the microhardness of the composite coatings in this study was slightly lower. M.H. Allahyarzadeh *et al*. [22] found that the hardness of the composite coating increased with increasing content of nanoparticles in the coating. Combined with the EDS results, it was not difficult to explain that the lower content of nanoparticles in composite coatings was a factor for the lower microhardness. In addition, heat treatment may also be another factor [23].

The presence of nanoparticles in the composite coatings increased the microhardness. In contrast, the presence of nanoparticles increases the nucleation point to reduce the grain size, and can hinder the movement of dislocations and the generation of plastic deformation [24]. The microhardness of composite coating containing ZrO_2 nanoparticles further improved, because of the high hardness and high strength of ZrO_2 particles, attributing higher microhardness to Ni–W–ZrO_2 composite coating than that of Ni–W–Y_2O_3 composite coating.

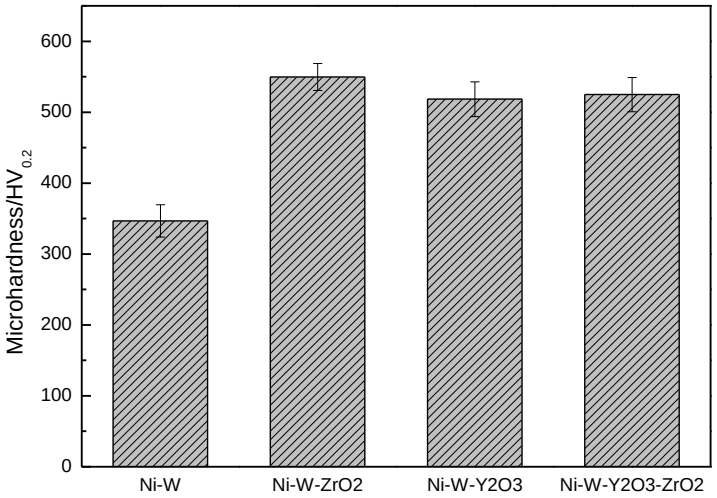

Figure 4. Microhardness of Ni–W alloy coating and Ni–W composite coatings containing ZrO_2 and Y_2O_3

3.4. Corrosion study

The electrochemical polarization curves and AC impedance of different composite coatings were measured in 3.5 wt% NaCl solution to study the difference in the corrosion resistance. The impedance spectrum of composite coatings and the equivalent circuit diagram were shown in Fig. 5(a),

where R_s represents the solution resistance, CPE represents the phase element between solution and the coating, and R_p is the electrochemical reaction charge transfer resistance. A semicircular capacitive impedance arc was observed as shown in Fig. 5(a). The capacitive impedance arcs of composite coatings containing nanoparticles were larger than that of Ni–W alloy coating, indicating that the corrosion resistance of the composite coatings was better than that of the alloy coating. The radius of Ni–W–Y_2O_3–ZrO_2 composite coating was the largest, i.e., the corrosion resistance was the best. The fitting data of impedance spectroscopy were listed in Table 4. The results were in agreement with the impedance spectra. The difference in the R_s value was very small; however, the R_p value of Ni–W–Y_2O_3–ZrO_2 composite coating was the largest, indicating that the charge transfer was the most difficult and the corrosion resistance was the best. The increase in the corrosion resistance of nanoparticles composite coatings was because of the fact that nanoparticles increased the nucleation point and reduced the grain size, thus hindering the corrosive medium from entering the composite coatings [25]. Y_2O_3 nanoparticle has a high corrosion resistance; therefore, the corrosion resistance of the composite coatings containing Y_2O_3 particles further improved. This was also the reason for better corrosion resistance of Ni–W–Y_2O_3 composite coating than that of Ni–W–ZrO_2 composite coating.

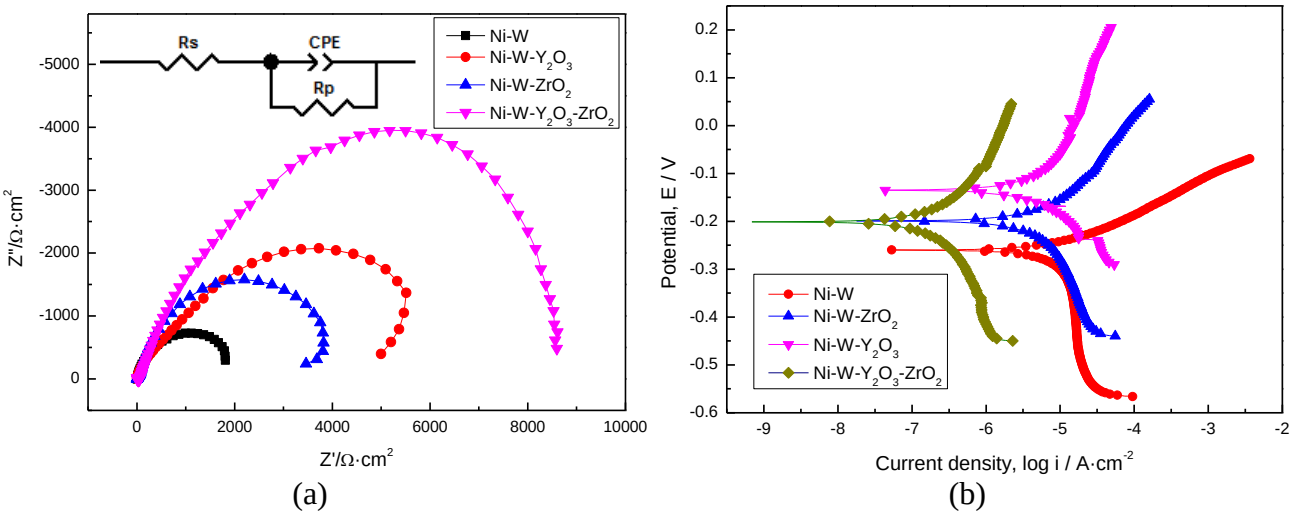

Figure 5. (a) Impedance spectra (b) Polarization curves of different coatings in 3.5% NaCl solution

Table 4. Electrochemical impedance data of Ni–W alloy coating and Ni–W composite coatings containing ZrO_2 and Y_2O_3

	R_s (Ω•cm^2)	R_p (Ω•cm^2)	CPE-T (Ω^{-1}•cm^{-2}•s^{-n})	CPE-P (Ω^{-1}•cm^{-2}•s^{-n})
Ni–W	3.74	2320	0.0007658	0.74
Ni–W–ZrO_2	3.02	4144	0.0002404	0.84
Ni–W–Y_2O_3	5.59	5611	0.0000709	0.78
Ni–W–Y_2O_3–ZrO_2	3.76	9507	0.0000489	0.85

The potentiodynamic polarization curves were shown in Fig. 5(b), and the fitting data were listed in Table 5. E_{corr} is the corrosion potential, showing the tendency to corrosion, and i_{corr} is the

corrosion current density, indicating the corrosion rate. The results of polarization curve were consistent with that of the impedance spectroscopy results. The corrosion potential of the composite coatings after adding nanoparticles increased obviously, decreasing the corrosion tendency. The corrosion current density decreased, indicating a lower corrosion rate. The self-corrosion current density of Ni–W–Y_2O_3–ZrO_2 composite coating was the lowest, indicating the lowest corrosion rate and the best corrosion resistance.

Table 5. Potentiodynamic polarization curve fitting data of Ni–W alloy coating and Ni–W composite coatings containing ZrO_2 and Y_2O_3

	b_a (mV/decade)	b_c (mV/decade)	i_{corr} (A/cm^2)	E_{corr} (V)
Ni–W	81.79	-1612.4	1.32E-05	-0.26
Ni–W–ZrO_2	180.36	-410.12	7.04E-06	-0.19
Ni–W–Y_2O_3	302.8	-176.56	5.44E-06	-0.13
Ni–W–Y_2O_3–ZrO_2	265.16	-418.33	3.27E-07	-0.20

4. CONCLUSION

In this study, ZrO_2 and Y_2O_3 nanoparticles were added into the plating solution to prepare composite coatings. The SEM, EDS, microhardness, and electrochemical tests of the composite coatings containing nanoparticles were performed. The EDS results showed that insoluble ZrO_2 and Y_2O_3 nanoparticles in the plating solution can be co-deposited with nickel ions during the composite electrodeposition process to form a composite coating. Compared to the electromagnetic stirring, the surface of the composite coating prepared under ultrasonic stirring condition was more dense and uniform, and no cracks were generated. The addition of ZrO_2 or Y_2O_3 nanoparticles improved the microhardness and corrosion resistance of the composite coating. When ZrO_2 and Y_2O_3 nanoparticles were added together, the microhardness of the composite coating slightly decreased, while the corrosion resistance of the composite coating significantly improved.

References

1. F. Bahrami, R. Amini and A.H. Taghvaei, *J. Alloys Compd.*, 714 (2017) 530.
2. F. Li, J. Cheng, S. Zhu, J. Hao, J. Yang and W. Liu, *Mater. Sci. Eng., A,* 682 (2017) 475.
3. C. Wang, Z. Farhat, G. Jarjoura, M.K. Hassanb, A.M. Abdullahb and E.M. Fayyadb, *Surf. Coat. Technol.*, (2017).
4. V. Vitry and L. Bonin, *Electrochim. Acta*, 243 (2017) 7.
5. M.R. Gorji, C. Edtmaier and S. Sanjabi, *Mater. Des.*, 125 (2017) 167.
6. P. Bacal, M. Donten and Z. Stojek, *Electrochim. Acta*, 241 (2017) 449.
7. A.L.M. Oliveira, J.D. Costa, M.B. Sousa, J.J.N. Alves, A.R.N. Campos, R.A.C. Santana and S. Prasad, *J. Alloys Compd.*, 619 (2015) 697.
8. A.R. Shetty and A.C. Hegde, *Surf. Coat. Technol.*, 322 (2017) 99.

9. A. Bigos, E. Beltowska-Lehmana, E. García-Lecinab, M. Biedaa, M.J. Szczerbaa and J. Morgiela, *J. Alloys Compd.*, (2017).
10. A. Góral, *Surf. Coat. Technol.*, 319 (2017) 23.
11. A. Bigos, E. Beltowska-Lehman and M. Kot, *Surf. Coat. Technol.*, 317 (2017) 103.
12. M. Nanko, M. Yoshimura and T. Maruyama, *Mater. Trans.*, 44 (2003) 736.
13. E. Beltowska-Lehman, P. Indyka, A. Bigos, M.J. Szczerba, J. Guspiel, H. Koscielny and M. Kot, *Mater. Chem. Phys.*, 173 (2016) 524.
14. Y. Xue, C. Shen, J. Li and Y. Liu, *Key Eng. Mater.*, 455 (2011) 427.
15. Y. Xue, C. Shen, J. Li, H. Li and D. Si, *Adv. Mater. Res.*, 97-101 (2010) 1235.
16. A. Nevers, L. Hallez, F. Touyeras and J. Hihn, Ultrason. Sonochem., (2017).
17. L Zhu, O Younes, N Ashkenasy, Y. Shacham-Diamand and E. Gileadi, *Appl. Surf. Sci.*, 200 (2002) 1.
18. S.A. Ataie and A. Zakeri, *J. Alloys Compd.*, 674 (2016) 315.
19. E. Beltowska-Lehman, P. Indyka, A. Bigos, M.J. Szczerba and M. Kot, *J. Electroanal. Chem.*, 775 (2016) 27.
20. L. Tian and J. Xu, *Appl. Surf. Sci.*, 257 (2011) 7615.
21. K.M. Sivaraman, O. Ergeneman, S. Pané, E. Pellicer, J. Sort, K. Shou, S. Suriñach, M.D. Baró and B.J. Nelson, *Electrochim. Acta*, 56 (2011) 5142.
22. M.H. Allahyarzadeh, M. Aliofkhazraei, A.R. Sabour Rouhaghdam and V. Torabinejad, *J. Alloys Compd.*, 666 (2016) 217.
23. M.V.N. Vamsi, N.P. Wasekar and G. Sundararajan, *Surf. Coat. Technol.*, 319 (2017) 403.
24. H. Li, Y. He, T. He, D. Qing, F. Luo, Y. Fan and X. Chen, *J. Alloys Compd.*, 704 (2017) 32.
25. B. Li, W. Zhang, W. Zhang and Y. Huan, *J. Alloys Compd.*, 702 (2017) 38.

© 2017 The Authors. Published by ESG (www.electrochemsci.org). This article is an open access article distributed under the terms and conditions of the Creative Commons Attribution license (http://creativecommons.org/licenses/by/4.0/).